Scheme I

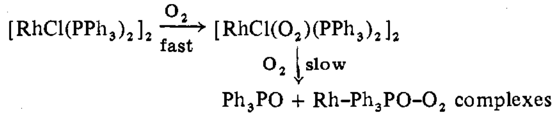

$$[RhCl(PPh_3)_2]_2 \xrightarrow[\text{fast}]{O_2} [RhCl(O_2)(PPh_3)_2]_2 \xrightarrow[\text{slow}]{O_2} Ph_3PO + Rh\text{-}Ph_3PO\text{-}O_2 \text{ complexes}$$

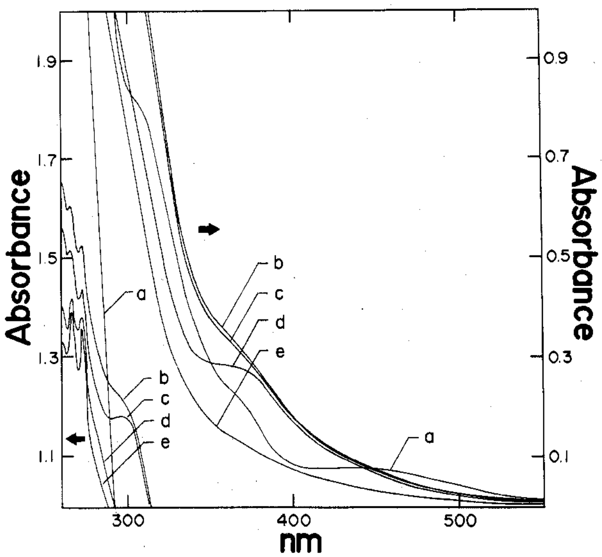

Figure 3. Electronic absorption spectral changes following exposure of a degassed $CH_2Cl_2$ solution of $[RhCl(PPh_3)_3]$ to air. Spectrum (a) was recorded prior to exposure and spectra (b–e) at the following time intervals after exposure: (b) immediately; (c) 15 min; (d) 4.3 h; (e) 25 h.

and Donaldson.[7] In $CH_2Cl_2$ solution their complex shows an absorption band at 366 nm, identical in position and shape to the spectrum resulting from the initial rapid reaction of $[RhCl(PPh_3)_2]_2$ with $O_2$. Further, storage of solutions of this dioxygen adduct gave infrared and electronic absorption spectral changes identical with and on the same time scale as those obtained under similar conditions during the oxidation of $[RhCl(PPh_3)_2]_2$.

A red-brown powder can be isolated from solutions of $[RhCl(PPh_3)_2]_2$ which have been exposed to oxygen for several days by precipitation with $Et_2O$ or by solvent evaporation. This powder can be reprecipitated from $CH_2Cl_2/Et_2O$ solutions, but a crystalline sample has not been obtained. The UV spectrum of this product in $CH_2Cl_2$ solution is identical with the final spectrum obtained from exposure of $[RhCl(PPh_3)_2]_2$ solutions to oxygen, and the IR spectrum shows bands at 1185 and 1118 $cm^{-1}$, assignable to $Ph_3PO$, and a band at 850 $cm^{-1}$ attributable to coordinated $O_2$. Satisfactory elemental analysis corresponding to any reasonable stoichiometry has not been obtained even though several carefully washed and reprecipitated samples were analyzed.

The spectral changes detailed above for $[RhCl(PPh_3)_2]_2$ and $[RhCl(O_2)(PPh_3)_2]_2$ indicate that oxidation of $[RhCl(PPh_3)_2]_2$ proceeds by very rapid formation of Bennett and Donaldson's dioxygen adduct, or an adduct which derives from their complex in solution, which then slowly decomposes to form $Ph_3PO$ and $Rh\text{-}Ph_3PO\text{-}O_2$ complexes, Scheme I. Since $[RhCl(PPh_3)_2]_2$ has been shown[12,13] to not dissociate to three-coordinate $[RhCl(PPh_3)_2]$ to any significant extent in solution, the initial fast reaction must occur between $O_2$ and the dimer. The slow decomposition to $Ph_3PO$ most likely proceeds through an intramolecular process similar to that proposed[14] for the $[Pt(PPh_3)_4]$ catalyzed oxidation of $PPh_3$.

The spectral changes which obtain during oxidation of $[RhCl(PPh_3)_3]$ are similar to those observed for $[RhCl(PPh_3)_2]_2$. A degassed $7 \times 10^{-5}$ M $CH_2Cl_2$ solution of $[RhCl(PPh_3)_3]$ shows an absorption band at 445 nm which upon exposure to $O_2$ is rapidly replaced by an absorption shoulder at 365 nm, Figure 3. This shoulder over a period of hours decreases in intensity and $Ph_3PO$ features simultaneously appear near 270 nm. The infrared spectral changes are virtually identical with those observed for $[RhCl(PPh_3)_2]_2$. Although the spectral changes obtained for the two complexes are similar, the relatively lower intensity of the 365-nm shoulder in the spectrum resulting from the reaction of $[RhCl(PPh_3)_3]$ with $O_2$ suggests that the oxidation pathways may not be entirely the same. Further, the very rapid initial reaction of $[RhCl(PPh_3)_3]$ with $O_2$ and our observation that a fivefold excess of $PPh_3$ does not inhibit the oxidation indicate that the reaction does not proceed entirely through $[RhCl(PPh_3)_2]_2$, and direct reaction of $O_2$ with $[RhCl(PPh_3)_3]$ is suggested.

Finally, we have observed that the oxidation products of $[RhCl(PPh_3)_3]$ and $[RhCl(PPh_3)_2]_2$ can be readily converted back to $[RhCl(PPh_3)_3]$ simply by refluxing ethanol solutions of the products with excess $PPh_3$ under a nitrogen atmosphere.

**Acknowledgment.** We thank the donors of the Petroleum Research Fund, administered by the American Chemical Society, and the National Science Foundation (Grant MPS 7505909) for support of this research.

**Registry No.** $[RhCl(PPh_3)_2]_2$, 14653-50-0; $[RhCl(PPh_3)_3]$, 14694-95-2; $O_2$, 7782-44-7.

## References and Notes

(1) M. C. Baird, D. N. Lawson, J. T. Mague, J. A. Osborn, and G. Wilkinson, *Chem. Commun.*, 129 (1966).
(2) R. L. Augustine and J. F. Van Peppen, *Chem. Commun.*, 495, 571 (1970).
(3) H. van Bekkum, F. van Rantwijk, and T. van de Putte, *Tetrahedron Lett.*, 1 (1969).
(4) K. W. Barnett, D. L. Beach, D. L. Garin, and L. A. Kaempfe, *J. Am. Chem. Soc.*, **96**, 7127 (1974).
(5) K. Takao, M. Wayaku, Y. Fujiwara, T. Imanaka, and S. Teranishi, *Bull. Chem. Soc. Jpn.*, **43**, 3898 (1970).
(6) K. Takao, M. Wayaku, Y. Fujiwara, T. Imanaka, and S. Teranishi, *Bull. Chem. Soc., Jpn.*, **45**, 1505 (1972).
(7) M. J. Bennett and P. B. Donaldson, *J. Am. Chem. Soc.*, **93**, 3307 (1971).
(8) R. L. Augustine and J. F. Van Peppen, *Chem. Commun.*, 497 (1970).
(9) C. W. Dudley, G. Read, and P. J. Walker, *J. Chem. Soc., Dalton Trans.*, 1926 (1974).
(10) G. L. Geoffroy, D. A. Denton, M. E. Keeney, and R. R. Bucks, *Inorg. Chem.*, **15**, 2382 (1976).
(11) J. A. Osborn and G. Wilkinson, *Inorg. Synth.*, **10**, 67 (1967).
(12) C. A. Tolman, P. Z. Meakin, D. L. Lindner, and J. P. Jesson, *J. Am. Chem. Soc.*, **96**, 2762 (1974).
(13) J. Halpern and C. S. Wong, *J. Chem. Soc., Chem. Commun.*, 629 (1973).
(14) J. P. Birk, J. Halpern, and A. L. Pickard, *J. Am. Chem. Soc.*, **90**, 4491 (1968).

---

Contribution from the Departments of Chemistry,
Baylor University, Waco, Texas 76703, and
University of Houston, Houston, Texas 77004,
and Brookhaven National Laboratory, Upton, New York 11973

## Crystal Structure of $Cs_2LiFe(CN)_6$ by Neutron Diffraction

G. W. Beall,[1a] W. O. Milligan,*[1a] J. Korp,[1b] I. Bernal,[1b]
and R. K. McMullan[1c]

*Received June 7, 1976* AIC60416V

The structure of a series of isomorphous compounds of the general formula $Cs_2LiM(CN)_6$, where M = Mn, Fe, and Co, has been determined.[2] These studies suggested a relation between the M–C bond distance and the amount of $\pi$ back-bonding. It was found that the $\sigma$ and $\pi$ contributions affected the M–C bond by approximately the same amount. The high symmetry of the crystals of these salts has also permitted a detailed vibrational analysis.[3,4] Since these salts do not suffer any of the disorder problems associated with other Prussian Blue analogues[5,6] and since the high symmetry

**Table I.** Final Least-Squares Parameters for $Cs_2LiFe(CN)_6$ from Neutron and X Ray[2]

| | $X$ | $\beta_{11}{}^a$ | $\beta_{22}$ | $\beta_{33}$ | $B$(Li) | $B$(Cs) | $B$(Fe) |
|---|---|---|---|---|---|---|---|
| Neutron | | | | | | | |
| C | 0.1823 (3) | 64 (2) | 64 (2) | 26 (3) | 1.93 (53) | 2.72 (12) | 1.22 (10) |
| N | 0.2907 (2) | 133 (3) | 133 (3) | 33 (3) | | | |
| X ray | | | | | | | |
| C | 0.1822 (3) | 63 (2) | 63 (2) | 41 (2) | 2.21 (16) | 3.70 (1) | 1.36 (2) |
| N | 0.2908 (3) | 131 (3) | 131 (3) | 41 (2) | | | |

$^a$ All $\beta$'s $\times 10^{-4}$.

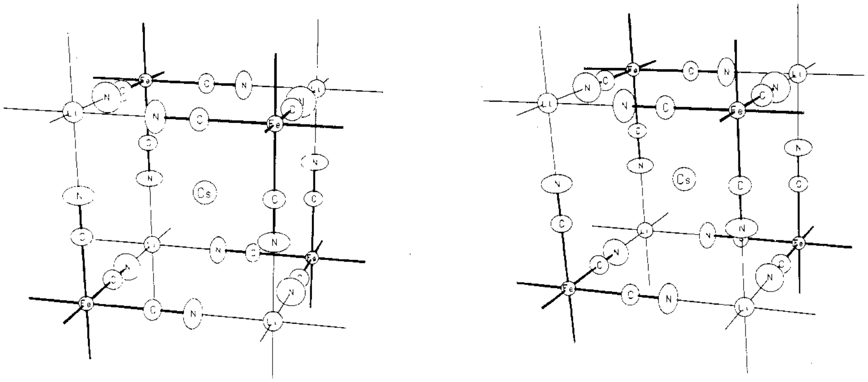

**Figure 1.** Arrangement of the atoms in the unit cell. Only one-eighth of the unit cell is shown in this figure.

eliminates problems associated with the low site symmetry[7,8] of the tripotassium salts $K_3M(CN)_6$, these factors made $Cs_2LiFe(CN)_6$ ideal to study the cyanide moiety with neutron diffraction. There are three major factors we are interested in: (1) the unambiguous determination of the carbon and nitrogen orientation relative to the iron, (2) the nuclear vs. electron cloud interatomic distances, and (3) the thermal parameters.

## Experimental Section

$Cs_2LiFe(CN)_6$ was prepared by combining aqueous solutions containing stoichiometric amounts of $Li_3Fe(CN)_6$ and $Cs_3Fe(CN)_6$. The tricesium and trilithium salts were synthezised from $K_3Fe(CN)_6$ by ion exchange on $Li^+$ and $Cs^+$ replaced hydrogen-form resin (Bio-Rad AG 50W-X16), and $K_3Fe(CN)_6$ was obtained commercially from Baker. The large crystals for neutron work were obtained by slow evaporation of aqueous solutions.

The data collection crystal was a dark red tabloid of approximate dimensions 3.0 × 2.8 × 1.8 mm. It was mounted on a glass capillary, with the [0 0 1] direction very nearly parallel to the $\phi$ axis of the diffractometer. A computer-controlled four-circle diffractometer at the Brookhaven National Laboratory High Flux Beam Reactor was used, with a wavelength of 1.383 Å selected by means of a Ge(III) monochromator crystal. Intensity data were collected at 24 °C, using a $\theta$:$2\theta$ step scan technique varying in width from 3.20 to 8.00° $2\theta$, out to a maximum of 105° $2\theta$. Six redundant zones were collected (the entire *hkl* octant). Three standard reflections (0, 4, 4; 6, 0, 0; and 2, 0, 0) were collected every 30 reflections, and no systematic variation in intensity was noted.

A Lorentz correction and an analytical absorption correction were applied to the data [$\mu$(neutrons) = 0.284 $cm^{-1}$]. The absorption correction factor ranged from 1.051 to 1.0%. The data were then averaged, with a residual error of 2.1%, to yield 76 unique reflections for the final refinement. The standard deviation of each individual reflection was determined from Poisson counting statistics. The standard deviations for the unique averaged data were calculated as follows:

$$\sigma_{\langle F\rangle}{}^2 = 1/n\Sigma(\sigma_{F_i}{}^2)$$

where $n$ = number of redundant reflections, and $\sigma_{F_i}{}^2$ = standard deviation for each redundant reflection.

**Refinement of Structure.** Wolberg's structure[10] was used as a starting model for full-matrix least-squares refinements. The accurate lattice constant found in the x-ray study[2] was used in this refinement owing to the difficulty encountered in obtaining lattice constants of this accuracy with the neutron diffractometer employed. The function minimized was $w^2\ (|F_o| - |F_c|)^2$, where $w^2$ is the weight defined as $1/\sigma^2(F_o)$.

**Table II.** Comparison of Interatomic Distances (Å) for $Cs_2LiFe(CN)_6$

| | Neutron | X ray[2] |
|---|---|---|
| Fe-C | 1.927 (3) | 1.926 (3) |
| Li-N | 2.212 (3) | 2.212 (3) |
| C-N | 1.146 (3) | 1.148 (5) |
| Cs-N | 3.805 (1) | 3.805 (1) |
| Cs-N | 3.762 (1) | 3.762 (1) |

The neutron scattering lengths used were $b$(Cs) = 0.55, $b$(Li) = −0.194, $b$(Fe) = 0.951, $b$(C) = 0.663, and $b$(N) = 0.940 cm (all $\times 10^{-12}$). The refinement converged after several cycles of full-matrix refinement[9] and application of a secondary extinction coefficient yielded an $R$ factor of 3.2% and an $R_w$ factor of 1.9%, where $R = \sum(|F_o| - |F_c|)/\sum|F_o|$ and $R_w = \sum w(|F_o| - |F_c|)/\sum w|F_o|$, where $w = 1/\sigma^2$. The carbon and nitrogen were refined anisotropically. A secondary extinction correction was also applied. The secondary extinction parameter $g$ was 2.3 (1) $\times 10^{-4}$.[11]

## Discussion

Table I shows a comparison of the least-squares parameters found in the neutron and x-ray studies.[2] The metals are all in special positions: Fe (0, 0, 0); Li, (0, 0, $^1/_2$); and Cs, ($^1/_4$, $^1/_4$, $^1/_4$). The isotropic thermal parameters for the Li and Fe are within $2\sigma$ in both studies, but there is a significant difference between the thermal coefficients for the Cs, with the neutron study yielding a significantly lower value.

The carbon and nitrogen positions relative to the Fe could be unambiguously determined since the neutron scattering factor for nitrogen is significantly larger than that for carbon. It can be seen that the positional parameters for the two studies are in complete agreement (carbon and nitrogen are in position set 24e; [0, 0, $x$]); however, the thermal parameters exhibit a significant difference. The thermal parameters perpendicular to the M–C bond, $\beta_{11}$ and $\beta_{22}$, are the same within one standard deviation. The difference comes in the thermal parameters along the cyanide bond, $\beta_{33}$, for which the neutron parameters are considerably smaller. A possible explanation is that it is a reflection of the amount of electron density contained in the cyanide bond, to which the x-ray study is sensitive.

**Table III.** Root-Mean-Square Amplitudes of Vibration (Å) for $Cs_2LiFe(CN)_6$ for Neutron and X Ray[2]

| | Neutron | X ray |
|---|---|---|
| Li | 0.156 (21) | 0.167 (12) |
| Cs | 0.185 (4) | 0.216 (1) |
| Fe | 0.125 (5) | 0.131 (2) |
| C(max) | 0.189 (3) | 0.188 (5) |
| C(min.) | 0.120 (8) | 0.153 (8) |
| N(max) | 0.272 (3) | 0.272 (6) |
| N(min.) | 0.135 (5) | 0.153 (8) |

Table II contains a comparison of bond distances for the neutron and x-ray studies. No peculiarities are noted. The structure is held together by the Li–N bond which agrees well with the sum of the crystal radii for Li and N of 2.1 Å.[12] The Cs atom seems to merely fill space and balance charge in the structure. The high thermal parameter of Cs would indicate that the hole containing it is too large. This is borne out by the fact that the distance between the Cs and nitrogen is 3.805 (1) Å, which is significantly larger than the sum of the crystal radii for Cs and N, 3.24 Å.[12] The C–N bond of 1.146 (3) seems to be an invariant distance in both the x-ray[2] and neutron refinements. In Table III a compilation of the root-mean-square amplitudes of vibration (Å) for both x rays and neutrons can be seen. Table IV compares observed and calculated crystal structure factors.

**Acknowledgment**. Two of us (J.K. and I.B.) acknowledge support from National Science Foundation Grant No. MPS-74-13718 and The Robert A. Welch Foundation Grant No. E-294. Two of us (G.W.B. and W.O.M.) acknowledge support in part from National Science Foundation Grant No. GH-34513. We wish to thank Dr. B. I. Swanson for the crystal employed in this study. Also, we thank Drs. G. Friedlander and G. A. Jeffrey of Brookhaven National Laboratory for allowing us to use the neutron diffraction facilities and for help during data collection.

**Registry No.** $Cs_2LiFe(CN)_6$, 37164-29-7.

**Supplementary Material Available**: Table of crystal structure factors (1 page). Ordering information is given on any current masthead page.

## References and Notes

(1) (a) Baylor University; (b) University of Houston; (c) Brookhaven National Laboratory.
(2) B. I. Swanson and B. R. Ryan, *Inorg. Chem.*, **12**, 286 (1973).
(3) B. I. Swanson and L. H. Jones, *J. Chem. Phys.*, **53**, 3761 (1970).
(4) B. I. Swanson and L. H. Jones, *J. Chem. Phys.*, **55**, 4174 (1971).
(5) A. Ludi, H. U. Gudel, and M. Ruegg, *Inorg. Chem.*, **9**, 2224 (1970).
(6) A. Ludi and H. U. Gudel, *Helv. Chim. Acta*, **51**, 2006 (1968).
(7) C. Gottfried and J. G. Nagelschmidt, *Z. Kristallogr., Kristallgeom., Kristallphys., Kristallchem.*, **73**, 357 (1930).
(8) J. A. Kohn and W. D. Townes, *Acta Crystallogr.*, **14**, 617 (1961).
(9) Computer programs used in this refinement were obtained from Los Alamos Scientific Laboratory Report LA-3043.
(10) A. Wolberg, *Acta Crystallogr., Sect. B.*, **25**, 161 (1969).
(11) A. C. Larson, *Acta Crystallogr.*, **23**, 664–665 (1967).
(12) J. C. Slater, *J. Chem. Phys.*, **41**, 3199 (1964).

---

Contribution from the Department of Chemistry, University of Victoria, Victoria, British Columbia, Canada V8W 2Y2

# Ligand Properties of *cis*-(Diphenylphosphinito)(hydroxydiphenylphosphine)platinum and -palladium Complexes

K. R. Dixon* and A. D. Rattray

*Received June 2, 1976* AIC60442T

Complexes in which there is the possiblity of a cis arrangement of one diphenylphosphinito[1] and one hydroxydiphenylphosphine ligand are known to exist as a symmetrical hydrogen bonded system of the type:

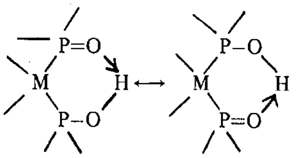

This was originally established by us on the basis of infrared evidence[3] and has since been confirmed by an x-ray diffraction study[4] of $[Pd_2(SCN)_2\{(PPh_2O)_2H\}_2]$. The reactivity of this type of system is of interest since if the proton can be replaced by other Lewis acids then a chelate ligand system somewhat analogous to acetylacetone is produced. Moreover, the overall result is a ligand bridging between "soft" and "hard" metal centers. The results described in the present note show that such proton replacement reactions are easily achieved and of general occurrence and suggest that the new ligand system will form a wide range of complexes analogous to the acetylacetonates. The presence of the spin $^1/_2$ phosphorus nucleus is of great assistance in structural studies and, in cases where the "hard" metal center is paramagnetic, the complexes can yield valuable data regarding the extent of electron delocalization.

Prior to our work, Austin reported reactions of $BF_3$ with $[PtCl_2(PPh_2OH)_2]$ and $[Pt\{PO(OCH_3)_2\}_2\{POH(OCH_3)_2\}_2]$ which yielded products similar to ours although the structures were not definitely established.[5] More recently, this type of reaction has been noted by Roundhill and co-workers,[2] who prepared three "$BF_2$ capped" complexes including one of those described below, namely $[Pt\{(PPh_2O)_2BF_2\}_2]$.

## Results and Discussion

Our most detailed studies have been carried out using the complex, $[PtCl(PEt_3)\{PPh_2O)_2H\}]$,[3] and Figure 1 shows the proton-decoupled $^{31}P$ NMR spectrum of this complex. Corresponding peak assignments and numerical data are collected in Table I, which also shows the proposed structure of the complex. The spectrum basically consists of two pairs of doublets, X and Z, centered at 129.0 and 64.5 ppm, respectively, and a triplet (Y) at 82.7 ppm. Each set of resonances is accompanied by satellites (X′, Y′ and Z′ in Figure 1) due to coupling to $^{195}Pt$ ($I = {}^1/_2$, relative abundance = 33.8%) and the assignments shown in Table I may be established on the basis of the platinum–phosphorus coupling constants. These are expected to be larger trans to Cl than trans to P and larger for phosphines having electron-withdrawing substituents (i.e., $PPh_2O > PEt_3$). This assignment then gives $J(P\text{–}P)_{trans} \gg J(P\text{–}P)_{cis}$, which is the expected order. The appearance of the $P_Y$ resonance as a triplet must be caused by overlap of peaks resulting from the very similar values of $J(P_X\text{–}P_Y)$ and $J(P_Y\text{–}P_Z)$, since a "deceptively simple" or "virtually coupled" X triplet is not expected in the ABX spin system for cases where $(\delta(A) - \delta(B)) > J(AB)$ (equivalent to $(\delta(X) - \delta(Z)) > J(P_X\text{–}P_Z)$ in the present complex).

Treatment of $[PtCl(PEt_3)\{(PPh_2O)_2H\}]$ with boron trifluoride etherate or with fluoroboric acid yields a colorless, crystalline solid analyzing as $[PtCl(PEt_3)\{(PPh_2O)_2BF_2\}]$ (see Table II). The $^{31}P$ NMR spectrum of this product (see Table I) is very similar to that shown in Figure 1 except for downfield shifts of all resonances, consistent with the introduction of an electron-withdrawing group and broadening of the $P_Y$ and $P_Z$ resonances caused by additional coupling to $^{10}B$, $^{11}B$, and $^{19}F$. The $^{19}F$ NMR spectrum is a broad ($W_{1/2} \sim 27$ Hz) single resonance showing some poorly resolved fine structure,[6] and the chemical shift (137.3 ppm upfield from $CFCl_3$) indicates the fluorine is bound to boron (cf. $BF_4^-$ at 147.5 ppm).[7] The compound $[PtCl(PEt_3)\{(PPh_2O)_2BF_2\}]$ is a nonelectrolyte in